CME LIVE OPEN ACCESS

Engineering and Applied Sciences Journal

Research Article

Formation-Evaporation of Germanium Monoxide in Water Vapor and Preparation of ($Ge+GeO_2$) Films

Nino Sepashvili[1], Zurab Adamia[2,3], Kokhreidze[1] and Irakli Nakhutsrishvili[1*]

[1]*Georgian Technical University, Tbilisi*

[2]*Sukhumi State University, Georgia*

[3]*Tbilisi State University, Georgia*

Corresponding Author: Irakli Nakhutsrishvili, Georgian Technical University, Tbilisi.

Received: 2024 Nov 09 **Accepted:** 2024 Nov 30 **Published:** 2024 Dec 07

Abstract

The reaction of oxidation of single-crystalline germanium in water vapor $Ge+H_2O=GeO+H_2$ is investigated. In this reaction ($Ge+H_2O=GeO+H_2$) the volatile germanium monoxide is formed. The kinetics of the reaction is studied using the microgravimetric method. GeO does not remain on the germanium surface and evaporates immediately. On a silicon substrate located in the cold zone of the reactor, the oxide disproportionate into germanium and its dioxide: $2GeO=Ge+GeO_2$. The infrared, electronic and Auger spectra of the ($Ge+GeO_2$) films were investigated. The capacitance-voltage characteristics were also measured. Film ($Ge+GeO_2$) creates a good interface with silicon. The breakdown voltage of the film under study reaches $\cong 2\cdot 10^7$ V/cm, which determines the prospects for its use in semiconductor devices for interlayer isolation.

Keywords: Germanium monoxide, Water vapor, Germanium suboxide film

1. Introduction

Oxide is grown on semiconductors to create MIS (metal-insulator-semiconductor) structures. Thermal oxidation is widely used for silicon. Thermal SiO_2 creates a high-quality interface with Si and other semiconductors. Germanium is similar to silicon in physical and chemical properties, surpassing it in charge carrier mobility. But its oxide layers do not have the qualities of silicon oxide. Nevertheless, germanium is widely used in microelectronics; it is used as an optical filter for IR radiation, a mirror resonator in lasers, a monochromator in diffractometers, memristors etc. [1-8].

When heated strongly, germanium reacts with oxygen to form oxides: momoxide GeO ($2Ge+O_2=2GeO$) or dioxide GeO_2 ($Ge+O_2=GeO_2$). These compounds are also formed by interaction of germanium with water vapor (does not react with liquid water) [9-11]: $Ge+H_2O=GeO+H_2$, $Ge+2H_2O=GeO_2+2H_2$.

Germanium monoxide is used in science and technology to no lesser extent than elemental germanium itself [12-29]. This paper examines the interaction of single-crystalline germanium with water vapor during the formation of monoxide and films obtained by evaporation of GeO.

1.1. Experimental

In the experiments, we used plates of single-crystalline germanium of n-type conductivity and with concentration of charge carriers $\cong 2\cdot 10^{14} cm^{-3}$. They were successively degreased in boiling toluene, dried in the air, etched in a liquid etchant HF-HNO3-CH3COOH = 1:15:1 for (4-5) min and, washed in running distilled water, followed by drying. The inlet pressure of water vapor was ≅2.64 kPa (saturated pressure of water vapor at 22 oC), which increased with the reaction temperature.

We studied the kinetics of the reaction using the microgravimetric method: the weighing of the change of the sample (sensitivity $\cong 10^{-6}$g). the monoxide vaporized from the germanium surface was applied to the silicon plate in the "cold" (300-350 oC) zone of the reactor. The germanium “suboxide” film obtained on the substrate was studied by infrared spectra (spectrophotometer UR-20), electronic absorption spectra (spectrophotometer SF-26-A), Auger-spectroscopic method (spectrometer LAS-2000) and measurement of capacitance - voltage (C-V) dependence (IPPM – 2 setup). To determine of charge built in dielectric (N_{FB}) and flat-band voltage (VFB), the high-frequency CV-characteristic method was used. The breakdown voltage of the films was measured using the AMI-60 apparatus.

2. Results and Discussion

Monoxide formed in the water vapor does not remain on the germanium surface and evaporates immediately. A study of the process by microgravimetry showed a linear decrease in the sample mass (Fig.1). According to dependencies m - t, it is possible to determine the evaporation rates of GeO at different temperatures, which is shown in Fig. 2 in Arrhenius coordinates. The experimental points strictly lie on a straight line and give the value of the activation energy ≅48 kcal/

mol, which is in satisfactory agreement with the literature data for the heat of evaporation of GeO (45-58) kcal/mol in different inert areas (Ar, N_2, vacuum) [30,31].

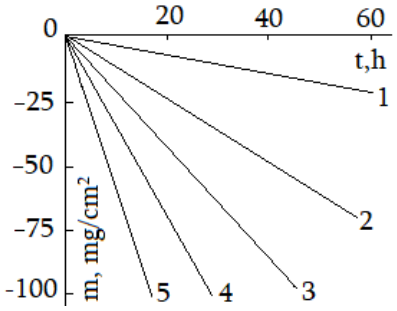

Figure 1: Mass loss of germanium sample in water vapor at (1) 500, (2) 550, (3) 600, (4) 650 and (5) 700°C.

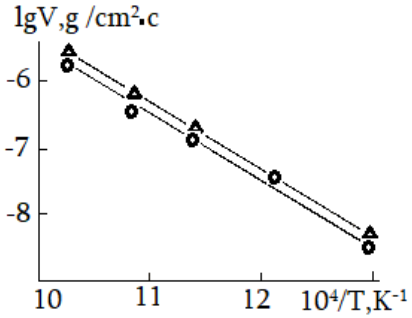

Figure 2: Temperature dependence of GeO evapioration in Arrheniuss coordinates in water vapor (o) and vacuum according to our data (Δ).

The vaporized GeO was applied to the silicon plate and infrared (IR), electron absorption and Auger spectra were studied. The volt-farad (C – V) characteristics were also investigated.

For films obtained in the temperature range of (500-700) °C, the optical properties change little. Thus, the maximum of the IR absorption spectrum is located in the region of (880-890) cm^{-1}, which is typical for GeO_2 [32,33], and the optical band gap (E_{opt}) (see below) lies within the limits of (1.2-1.3) eV, which is already approaching E_{opt} for amorphous germanium [34,35].

Comparison of the IR spectrum and the band gap width suggests a two-phase structure of the films. Direct evidence of this is the Auger spectrum (Fig.3, curve 1). The Auger spectra of amorphous GeO_2 (curve 2) and Ge (curve 3) films are also shown there. In the film under study, the peak of the LMM transition of germanium is split into two components with energies of 1140 and 1147 eV. The first corresponds to the Auger transition of germanium atoms in Ge(O_4) tetrahedra in GeO_2, and the second - in Ge (Ge_4) tetrahedra. (*)

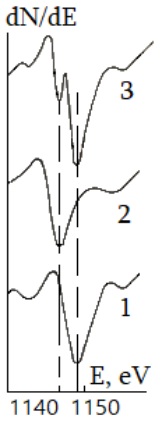

Figure 3: Auger-spectrum of (1) Ge, (2) GeO_2 and (3) Ge+GeO_2 film.

Thus, it should be concluded that when deposited on the substrate, GeO disproportionate: 2GeO = Ge +GeO_2. It should be noted that this two-phase nature is not a trivial fact - **GeO_2** films obtained by magnetron and triode sputtering of germanium are single-phase. (**)

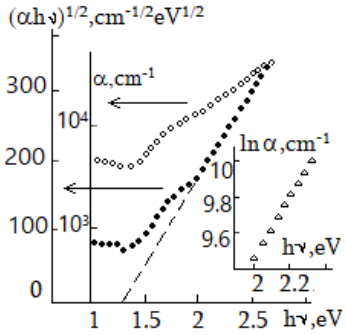

Figure 4: Electronic absorption spectra of Ge+GeO_2 film obtained by at 700°C in different coordinates.

Figure 4 shows the electronic absorption spectrum of the film obtained at 700°C in the coordinates absorption coefficient (α) - photon energy (hν, h - Plank's constant, ν - frequency), (αhν)1/2 - hν and lnα - hν. To describe the presented dependencies, one can use known equations: αhν=B(hν-Eopt)2 [36,37] and α=α0exp(hν/E0) [38-40], where B is a coefficient inversely proportional to the density of states near the conduction band and valence band, α0 is the pre-exponent and E0 is the Urbach's energy. The Urbach's "tail of states" is associated with defects caused by the violation of the long-range ordering of the structure in amorphous materials [41,42].

The properties of the interface of the obtained films with silicon were investigated. Fig. 5 shows the C-V characteristic of the Al-(Ge+GeO_2)-Si structure based on the film obtained at 700 °C. It has a hysteresis of (1-2) V and a counterclockwise direction. The latter indicates ion drift in the material [43]. Flat band voltage V_{FB}=2V, which indicates the predominance of a negative fixed charge (density $N_{FB}=2.6\cdot10^{11}$ cm^{-2}).

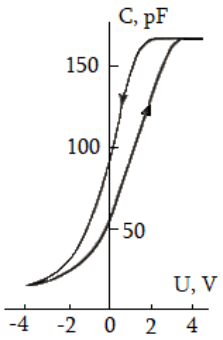

Figure 5: C - V characteristic of structure (Ge+GeO_2) – Si.

The breakdown voltage of the film reaches 2·107 V/cm. This high value determines the prospects for using the (Ge+**GeO_2**) film for interlayer insulation in semiconductor devices.

2.1. Footnotes

(*) It is known that many oxides, especially **GeO_2**, dissociate with the release of oxygen under electron or ion irradiation. This may cause a false signal of germanium. We prevented thermal destruction by reducing the energy of the primary beams (<2.5 keV) and decreasing the density of current.

(**) In the Auger spectra of homogeneous solid solutions of GeOx (0≤x≤2), a singlet peak is observed, the maximum of which shifts from 1140 to 1147 eV depending on x.

3. Conclusion

The reaction of oxidation of single-crystalline germanium in water vapor Ge+H_2O=GeO+H_2 is investigated, when volatile germanium monoxide is formed. GeO does not remain on the germanium surface and evaporates immediately. In the cold zone of reactor monoxide, it disproportionates into germanium and its dioxide 2GeO=Ge+GeO_2. Film (Ge+GeO_2) creates a good interface with silicon. The breakdown voltage of the film under study reaches ≅$2\cdot10^7$ V/cm, which determines the prospects for its use in semiconductor devices for interlayer isolation.

References

1. Duris, M., Deubel, D., Bodiou, L., Vaudry, C., Keromnes, et al. (2021). Fabrication of Ge-ZnS multilayered optical filters for mid-infrared applications. *Thin Solid Films*, 719, 138488.
2. Denker, B. I., Galagan, B. I., Sverchkov, S. E., Koltashev, V. V., Plotnichenko, V. G., et al. (2021). Resonantly pumped Ce 3+ mid-infrared lasing in selenide glass. *Optics Letters, 46*(16), 4002-4004.
3. Li, Y., Khounsary, A. M., Narayanan, S., Macrander, A. T., Khachatryan, R., et al. (2004, November). Design and analysis of a cooled Z-shaped germanium x-ray monochromator. In *X-Ray Sources and Optics* (Vol. 5537, pp. 189-192). SPIE.
4. Yushkov, I. D., Yin, L., Kamaev, G. N., Prosvirin, I. P., Geydt, P. V., et al. (2023). Memristors based on many-layer non-stoichiometric germanosilicate glass films. *Electronics,*

12(4), 873.
5. Zhang, F., Volodin, V. A., Astankova, K. N., Shvets, P. V., Goikhman, A. Y., et al. (2024). Kinetic study of GeOx amorphous film disproportionation into a-Ge nanoclusters/ GeO2 system using Raman and infrared spectroscopy. *Journal of Non-Crystalline Solids*, 631, 122929.
6. Waheed, H., Javaid, K., Ali, A., Mahmood, K., Arshad, M. I., et al. (2024). Band alignment engineering of p-Ge/n-Si heterojunction for low cost tandem solar cell applications. *Optical Materials*, 157, 116222.
7. Cheng, C. H., Chou, K. Y., Chin, A., Yeh, F. S. (2010, December). Very high-performance non-volatile memory on flexible plastic substrate. In 2010 *International Electron Devices Meeting* (pp. 21-5). IEEE.
8. Volodin, V. A., Kamaev, G. N., Gritsenko, V. A., Gismatulin, A. A., Chin, A., Vergnat, M. (2019). Memristor effect in GeO [SiO2] and GeO [SiO] solid alloys films. *Applied Physics Letters*, 114(23).
9. Sparnaay, M. J. (1963). The reaction between water vapor and the germanium surface. *Annals of the New York Academy of Sciences,* 101(3), 973-982.
10. Greenwood, N. N., Earnshaw, A. (2012). *Chemistry of the Elements*. Elsevier.
11. Jolly, W. L., Latimer, W. M. (1952). The equilibrium Ge (s)+ GeO2 (s)= 2GeO (g). The heat of formation of germanic oxide. *Journal of the American Chemical Society, 74*(22), 5757-5758.
12. Reedijk, J., Poeppelmeier, K. R. (2013). Comprehensive inorganic chemistry II: from elements to applications.
13. Khatoon, N., Subedi, B., Chrisey, D. B. (2024). Synthesis of Silicon and Germanium Oxide Nanostructures via Photonic Curing; a Facile Approach to Scale Up Fabrication. *ChemistryOpen*, e202300260.
14. Tiama, T. M., Ibrahim, M. A., Sharaf, M. H., Mabied, A. F. (2023). Effect of germanium oxide on the structural aspects and bioactivity of bioactive silicate glass. *Scientific Reports, 13*(1), 9582.
15. Ghaithaa, H., Kamaev Gennadiy, N., Michel, V., Volodin Vladimir, A. (2024). Photocurrent in MIS structures based on germanosilicate films. *St. Petersburg Polytechnic University Journal: Physics and Mathematics, 72*(1.1), 149-154.
16. Konstantinov, V. O., Baranov, E. A., Fan, Z., Shchukin, V. G., Zamchiy, A. O., Volodin, V. A. (2024). Formation of Germanium Nanocrystals and Amorphous Nanoclusters in GeO [SiO] and GeO [SiO 2] Films Using Electron Beam Annealing. *Technical Physics, 69*(4), 898-905.
17. Fukuda, Y., Otani, Y., Itayama, Y., Ono, T. (2007). Electrical analyses of germanium MIS structure and spectroscopic measurement of the interface trap density in an insulator/ germanium interface at room temperature. *IEEE transactions on electron devices, 54*(11), 2878-2883.
18. Alenizi, M. A., Aouassa, M., Bouabdellaoui, M., Saron, K. M. A., Aladim, A. K. et al. (2024). Electrical and dielectric characterization of Ge quantum dots embedded in MIS structure (AuPd/SiO2: Ge QDs/n-Si) grown by MBE. *Physica* B: *Condensed Matter*, 685, 415962.
19. Zang, H. J., Kim, G. S., Park, G. J., Choi, Y. S., Yu, H. Y. (2016). Asymmetrically contacted germanium photodiode using a metal–interlayer–semiconductor–metal structure for extremely large dark current suppression. *Optics Letters,* 41(16), 3686-3689.
20. Liu, P., Le, S. T., Lee, S., Paine, D., Zaslavsky, A., et al. (2012, August). Fast, high-efficiency Germanium quantum dot photodetectors. In 2012 *Lester Eastman Conference on High Performance Devices* (LEC) (pp. 1-3). IEEE.
21. Shalimova, M.B., I. V. Belyanina, I.V. (2023). Changing the parameters of MIS structures with REE compounds under conditions of high humidity. Semiconductors, 2, 85.
22. Du, S. J., Li, X. X., Tian, Y., Liu, Y. Y., Jia, K., et al. (2024). Analyzing the surface passivity effect of germanium oxynitride: a comprehensive approach through first principles simulation and interface state density. *Nuclear Science and Techniques, 35*(5), 45.
23. Shimazaki, E., Matsumoto, N., Niwa, K. (1957). The vapor pressure of germanium dioxide. *Bulletin of the Chemical Society of Japan, 30*(9), 969-971.
24. Barton, L., Heil, C. A. (1970). The reduction of germanium dioxide with graphite at high temperatures. *Journal of the Less Common Metals, 22*(1), 11-17.
25. Pauleau, Y., Remy, J. C. (1975). Kinetics of the formation and sublimation of germanium monoxide. *Journal of the Less Common Metals, 42*(2), 199-208.
26. Khan, M. A., Farhan, M., Hogan, T. P. (2009, June). Low temperature synthesis of germanium oxide nanowires by thermal evaporation of germanium in an oxidizing environment. In 2009 *IEEE Nanotechnology Materials and Devices Conference* (pp. 5-8). IEEE.
27. Astankova, K. N., Volodin, V. A., Azarov, I. A. (2020). Structure of germanium monoxide thin films. *Semiconductors*, 54(12), 1555-1560.
28. Kadomtseva, A. V., Mochalov, G. M., Zasovskaya, M. A., Ob'edkov, A. M. (2024). Synthesis, Structure, and Biological Activity of the Germanium Dioxide Complex Compound with 2-Amino-3-Hydroxybutanoic Acid. *Inorganics, 12*(3), 83.
29. Filella, M., May, P. M. (2023). The aqueous solution chemistry of germanium under conditions of environmental and biological interest: Inorganic ligands. *Applied Geochemistry,* 155, 105631.
30. Inoue, M. (1972). Etching of germanium with water vapor. Japanese *Journal of Applied Physics, 11*(8), 1147.
31. Arslambekov, V.A., Rozhansky, N.V. (1983). Kinetics of interaction of germanium surface with oxygen and evaporation of formed oxides in vacuum. Surface, 3, 95.
32. Teredesai, P. V., Anderson, D. T., Hauser, N., Lantzky, K., Yarger, J. L. (2005). Infrared spectroscopy of germanium dioxide (GeO2) glass at high pressure. *Physics and chemistry of glasses, 46*(4), 345-349.
33. Zhang, F., Volodin, V. A., Astankova, K. N., Kamaev, G. N., Azarov, I. A., et al. (2022). Determination of the infrared absorption cross-section of the stretching vibrations of Ge–O bonds in GeOx films. *Results in Chemistry,* 4, 100461.
34. Liu, P., Longo, P., Zaslavsky, A., Pacifici, D. (2016). Optical bandgap of single-and multi-layered amorphous germanium ultra-thin films. *Journal of Applied Physics, 119*(1).
35. Clark, A. H. (1967). Electrical and optical properties of amorphous germanium. *Physical Review, 154(*3), 750.
36. Toudert, J., Serna, R. (2017). Interband transitions in semi-metals, semiconductors, and topological insulators: a new

driving force for plasmonics and nanophotonics. *Optical Materials Express, 7*(7), 2299-2325.
37. Ekimov, A. I., Safarov, V. I. (2023). Optical Orientation of Carriers in Interband Transitions in Semiconductors. *JETP Letters, 118*(Suppl 1), S38-S40.
38. Bala, K. J., Peter, A. J., Lee, C. W. (2019). Interband and intersubband optical transition energies in a Ga0. 7In0. 3N/GaN quantum dot. *Optik, 183*, 1106-1113.
39. Bala, K. J., Peter, A. J., Lee, C. W. (2019). Interband and intersubband optical transition energies in a Ga0. 7In0. 3N/GaN quantum dot. *Optik*, 183, 1106-1113.
40. Holovský, J., Ridzoňová, K., Peter Amalathas, A., Conrad, B., Sharma, R. K., et al. (2023). Below the Urbach Edge: Solar Cell Loss Analysis Based on Full External Quantum Efficiency Spectra. *ACS Energy Letters, 8*(7), 3221-3227.
41. Wang, L., Liu, B., Li, H., Yang, W., Ding, Y., et al. (2012). Long-range ordered carbon clusters: a crystalline material with amorphous building blocks. *Science, 337*(6096), 825-828.
42. An, C., Zhou, Y., Chen, C., Fei, F., Song, F., et al. (2020). Long-range ordered amorphous atomic chains as building blocks of a superconducting quasi-one-dimensional crystal. *Advanced Materials, 32*(38), 2002352.
43. Belanovsky, A.S., Baranov, G.D. (1968). Silicon nitride films. Reviews on Electronic Engineering - Semiconductor Devices, 15, 125.